V₈₃₀ AND FUNDAMENTAL SITE PERIOD ESTIMATES IN SOFT SEDIMENTS OF THE OTTAWA VALLEY FROM NEAR-SURFACE GEOPHYSICAL MEASUREMENTS

Beatriz Benjumea, Cartographic Institute of Catalonia, Barcelona, Spain James A. Hunter, Geological Survey of Canada, Ottawa, Ontario, Canada Susan E. Pullan, Geological Survey of Canada, Ottawa, Ontario, Canada Gregory R. Brooks, Geological Survey of Canada, Ottawa, Ontario, Canada Matt Pyne, Geological Survey of Canada, Ottawa, Ontario, Canada Janice M. Aylsworth, Geological Survey of Canada, Ottawa, Ontario, Canada

Abstract

Seismic techniques have been used to supplement geological and geophysical borehole data for assessing earthquake hazard in the Ottawa valley near Ottawa, Ontario, Canada. The methodology used to obtain critical parameters for site effect studies (depths of major contacts, shear-wave velocity function) is presented in this paper. Bedrock depth values and basic stratigraphic information were obtained from water well descriptions and three geological units were defined: post-glacial marine, deltaic and fluvial sediments (mainly silt, clay and sand), glacial sediments (till, glaciofluvial sand and gravel), and Paleozoic (limestone, shale) and Precambrian bedrock. In order to augment existing knowledge of bedrock depths and overburden stratigraphy, 100 P-wave reflection soundings (test sites) were acquired. Good quality, high-frequency data have allowed identification of the reflections associated with the glacial-post-glacial boundary as well as the top of bedrock at each site. Subsequently, P-wave and S-wave velocities measured from highresolution downhole logging in boreholes in the Ottawa Valley area have been used to establish Pand S-wave velocity functions for each stratigraphic unit. We have used these results to: 1) obtain thickness of unconsolidated post-glacial and glacial sediments and bedrock depth at the P-wave reflection sites, 2) calculate V_{s30} for all borehole and seismic test site locations and plot NEHRP site classifications over the study area, and 3) combine shear-wave velocity and depth/thickness information to obtain a fundamental resonance period map.

Introduction

Earthquake ground-motion amplification where soft sediments overlie hard bedrock is a major factor in assessing earthquake hazard (Aki, 1988, 1993). Since estimating site response relies on determining the extent that ground motion is modified by local geological conditions, it is critical to know the physical parameters and lateral variation of the immediate subsurface soils and bedrock. In particular, the shear wave velocity-depth function is essential to understanding the response of thick soils during earthquake shaking. It is common practice in civil engineering to focus on the average shear wave velocity to 30 m depth (Vs₃₀), which is used to define soil classification categories by the National Earthquake Hazard Reduction Program (NEHRP, 1994). The NEHRP classifications were adopted in seismic regulations for new buildings in the United States in 1998 (Building Seismic Safety Council (BSSC), 1998), and more recently have been adopted in the 2005 edition of the National Building Code of Canada (NBCC, Finn and Wightman, 2003). Table 1 gives the site classification for seismic site response as defined by NEHRP (1994). The shear wave velocity definition depends on the value of Vs₃₀, which is calculated from the time taken for shear waves to travel from a depth of 30 m up to the ground surface. That is:

$$V_{s_{30}} = (30/\text{ sum } [h/V_s])$$
 m/s (1)

where h and Vs represent the thickness (in m) and shear wave velocities (in m/sec), respectively, of the individual layers between the ground surface and 30 m depth (from Finn and Wightman, 2003).

Table 1: Vs₃₀ site classification for seismic site response as defined by NEHRP (1994). Adapted from Finn and Wightman, 2003.

Site Class	Description	Shear Wave Velocity Definition
A	Hard rock	$V_{s_{30}} > 1500 \text{ m/s}$
В	Rock	$760 \text{ m/s} < V_{s_{30}} < 1500 \text{ m/s}$
C	Very dense soil and soft rock	$360 \text{ m/s} < V_{S30} < 760 \text{ m/s}$
D	Stiff soil	$180 \text{ m/s} < V_{s_{30}} < 360 \text{ m/s}$
Е	Soil with soft clay	$V_{S30} < 180 \text{ m/s}$

Current techniques used to obtain shallow shear wave velocities (Vs) can be classified as either passive methods based on microtremor measurements (background noise recording), or methods using conventional seismic techniques with active and controlled seismic sources.

The use of conventional seismic techniques for determining shear wave velocities has been discussed by Hunter et al. (2002), who apply high-resolution shear wave refraction and reflection methods for measuring both vertical and lateral variations in shear wave velocities in the near-surface. To optimize these techniques, these authors recommend supplementing site-specific one-dimensional measurements with downhole velocity logging or the equivalent seismic cone penetrometer measurements. These downhole methods are considered to be the most reliable ones for vertical axis measurements of shear wave velocities.

The primary objective of this paper is to discuss and demonstrate the use of combined seismic and borehole data for deriving subsurface structure, Vs_{30} , and NEHRP classification maps for earthquake hazard assessment. The study area used in this demonstration is a 26x34 km area centred on the town of Bourget, approximately 50 km east of Ottawa, Ontario, Canada. It is an excellent field laboratory due to the presence of thick soft sediments overlying an irregular bedrock surface. Overburden structure can also vary considerably over short lateral distances. In addition, high-resolution geophysical velocity logs have been acquired in several boreholes from which a reliable shear wave velocity-depth function can be obtained (Hunter et al., 2006). Although the area is located in a moderate active earthquake seismic region (see below), it has been inferred to have been subjected to occasional high-magnitude earthquakes during the Holocene (Aylsworth et al., 2000; Adams and Halchuk, 2003).

As a secondary objective, a discussion about the implications of using the Vs₃₀ criteria in this example area, is presented.

Bourget Study Area

Geology

The Bourget study area (Fig. 1) is located in the Ottawa-St. Lawrence Lowlands, which were inundated by the Champlain Sea approximately 11,000 years ago (Fig. 1a). The study area is underlain by Paleozoic sedimentary rock that unconformably overlies Precambrian crystalline basement rock (Williams and Telford, 1986). Bedrock is exposed locally, but over much of the area it is buried by late Quaternary unconsolidated deposits of variable thickness (up to 187 m thick, see Figure 2). A number of irregularly-shaped depressions in the bedrock surface form closed basins (Fig. 2) that are buried beneath Quaternary deposits and lack surface expression (Fig. 1).

The Quaternary depositional sequence generally consists of gravel diamicton (till), glaciomarine silty clay, pro-delta silt and silty clay rythmites, and deltaic silt overlain by fluvial silty sand (Gadd, 1986). The depositional sequence reflects the presence of Laurentide glacial ice, inundation by the Champlain Sea following deglaciation (beginning ca. 11.5 ka BP), and fluvial sedimentation on the delta plain (Fulton and Richard, 1987). Following recession of the Champlain

Sea after ca. 10 ka BP, a proto-drainage network incised the delta plain, eroding several large, intersecting (paleo-) channels up to 6 km wide, as well as the river valleys occupied by the modern Ottawa and South Nation rivers (Fig. 1; Aylsworth et al., 2000).

The glaciomarine and pro-delta silt and silty-clay deposits are informally known as "Leda clay" and are composed of glacially-ground, non-clay minerals held together in a loose structural framework (Torrance, 1988). These deposits can be geotechnically "sensitive" and vulnerable to rapid failure generating large-scale, retrogressive earthflows (e.g. Eden et al., 1971; Evans and Brooks, 1994). For the purposes of this paper, the glaciomarine, deltaic and fluvial deposits will be referred to collectively as "post-glacial" deposits and the diamicton as "glacial" deposits. These distinctions are made to reflect differing shear wave velocity characteristics between post-glacial and glacial deposits as discussed below.

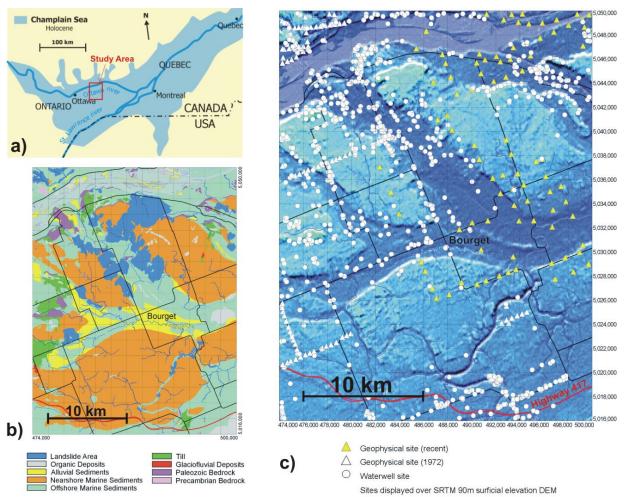


Figure 1: a) Location of the study area east of Ottawa, Ontario, Canada, showing the extent of the Champlain Sea deposits within the St. Lawrence Lowland. b) surficial geology of the study area, c) Locations of the borehole data and the recent seismic test sites (yellow triangles, shown on a shaded relief map. Topographic lows are associated with abandoned channels of the Ottawa River.

Seismic Activity

The Ottawa-Bourget area is subject to contemporary seismic activity from within two bands: the area underlying the Ottawa valley, and an area just to the east extending several hundred kilometers northwest of Montreal; together these bands form the West Quebec Seismic Zone (Adams and Basham, 1989). The occurrence of two major mid-Holocene earthquakes (>M6.5) in the lower Ottawa Valley has been inferred by Aylsworth et al. (2000), based upon the coincidental radiocarbon

ages of a cluster of large-scale earthflows in the Bourget area and the presence of a large area of fine-grained marine sediments and sand near Lefaivre, Ontario, which has experienced irregular surface subsidence, lateral spreading, and sediment deformation to a depth of 50 m.

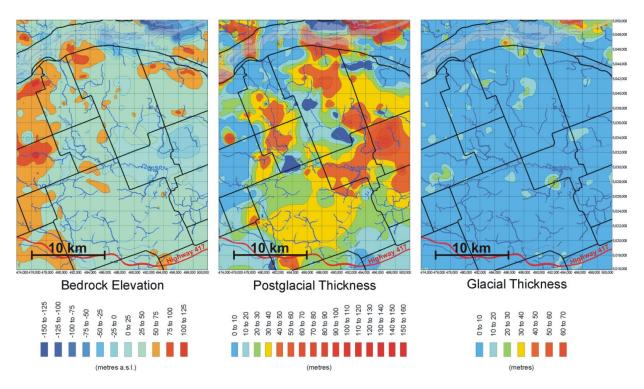


Figure 2: Maps of bedrock elevation and thickness of glacial and post-glacial sediments in the study area, produced from the combined borehole and geophysical data. Bedrock elevation varies from approximately 150 m below sea-level to 125 m above sea-level. Post-glacial sediments range from 0 to 160 m in thickness, with the thickest deposits found in the northeast corner of the study area and above bedrock depressions in the central eastern area. Glacial sediments lying on bedrock are relatively thin (<10 m) except for isolated locations where thick glacial sediments are associated with bedrock topographic lows and probably represent infilling of pre-existing bedrock valleys during the Pleistocene era.

Methodology

The methodologies applied to this study area include: 1) a revision of the water-well/borehole geological database, 2) the use of P-wave seismic reflection data to locate bedrock and other major acoustic impedance contrasts, 3) development of an average shear-wave velocity-depth function from the downhole seismic database, and 4) application of both depth and Vs_{av} functions to obtain Vs_{30} and NEHRP site classifications and fundamental site resonance period maps.

Borehole Database

Bedrock depth values and basic stratigraphy information from available borehole information defined the three basic geological units mentioned above: post-glacial deposits, glacial sediments, and bedrock.

The three-dimensional architecture of the unconsolidated deposits in the study area was first compiled by using the digital subsurface database of the Urban Geology of the National Capital Area website (http://gsc.nrcan.gc.ca/urbgeo/natcap/index_e.php; Belanger, 1998). The database contains only boreholes that reached bedrock and is comprised of 2370 engineering borehole logs, 23,192 water well logs, and 1610 refraction seismic sites; it was last updated in 1994. Individual borehole records contain information on each record (identification, location, surface elevation, bedrock depth) and generalized stratigraphic data (generic name of soil unit, lithology, adjective modifier,

depth, and thickness). The database is intended to be used for site-specific stratigraphic information and for the generation of maps and graphics at a regional scale.

Within the study area, the database consists of 700 water well records, 10 engineering logs, 100 outcrop observations, supplemented with data from 84 hammer seismic refraction sites surveyed in the 1970s (Fig. 1). Each data site was intersected with the surficial geology map to determine depositional environment. Sediments were determined to be either glacial or postglacial in origin based on lithology of the unit and inferred depositional environment. Geophysical sites without lithological information were assumed to be postglacial sediments over bedrock (since glacial deposits are known to be relatively thin or absent in most boreholes).. The sites were then intersected with the SRTM digital elevation model (DEM). Drift thickness was subtracted from surface elevation to create the bedrock elevation map.

Seismic Reflection Sites

In order to augment existing knowledge of bedrock depths and overburden stratigraphy, 100 P-wave reflection soundings (test sites) were acquired. Good quality, high-frequency data allow identification of the reflections associated with the glacial/post-glacial boundary as well as the top of bedrock at each site. The test sites were located in areas where data in the borehole database was sparse, which tended to be areas of thicker post-glacial and glacial sediments.

At each site, a 24-channel array of 50-Hz vertical geophones at 3 m spacing was laid out in the ditch alongside the road, and seismic records were obtained for shots in the centre of the spread, and at 3 and 4.5 m off each end. The compressional wave seismic source was a 12-gauge in-hole shotgun source or "Buffalo gun", which detonates a 180-grain blank, black-powder load at \sim 1 m depth in a shallow 4-cm diameter shothole. The seismic data were recorded with a Geometrics Strataview TM engineering seismograph.

Figure 3 shows an example of data acquired at test site 3. The raw field data from the shot at the centre of the spread (Fig. 3a) shows large amplitude, low frequency energy (<50 Hz), but also visible higher frequency reflection energy (e.g. at 80-100 ms). The low-frequency energy is easily removed by simple bandpass filtering (Fig. 3b), and high-frequency reflections (hyperbolic events) are then clearly visible. The entire suite of five records obtained at the site (with the geometry shown schematically in Fig. 3d) can be processed to produce a low-fold seismic section, which is a two-way traveltime image of the subsurface structure (Fig. 3c). The excellent reflection data quality shown in Figure 3 is typical of sites shot on Champlain Sea sediments (fine-grained, water-saturated sediments at surface) which provide an extremely favourable environment for generating and transmitting high-frequency seismic signals.

These data provide two-way travel times determined for reflections from the top of the glacial sediments (where observed) and the bedrock surface. Using the velocity information discussed in the following section, these travel times can be interpreted as depths, and used to supplement the information derived from the available borehole database.

Shear-wave velocity-depth function from downhole seismic data

Borehole geophysical logging has been carried out in 18 widely separated boreholes in Champlain Sea sediments in the Ottawa-Montreal area for other geotechnical and groundwater projects (Hunter et al., 2006). The suite of geophysical logs obtained in these boreholes includes P-and S-wave downhole velocity logs, acquired using the equipment and techniques described in Hunter et al. (1998), which provide the data needed to: 1) calculate accurate depths to bedrock and other major acoustic impedance contrasts from the seismic reflection data described above, and 2) estimate shear-wave velocity depth functions.

Most boreholes were drilled in mainly post-glacial sediments, and a review of the P-wave logs indicated that the compressional-wave velocities (Vp) below the water table in these sediments had a uniform value of 1500 m/s with little variation with depth. This value was therefore used to calculate depths to reflectors below the water table at all seismic sites.

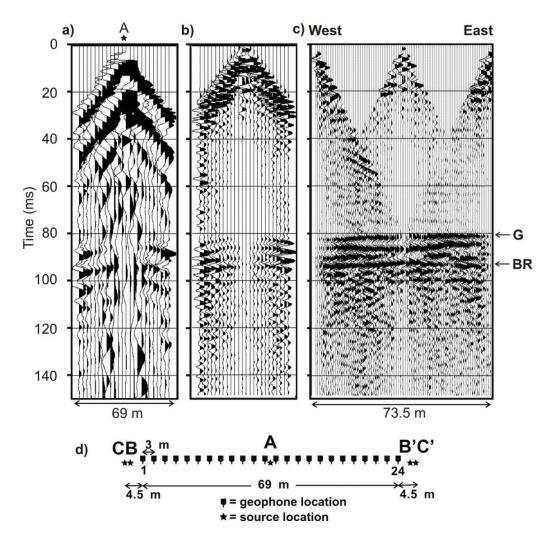


Figure 3: Example of test site data and processing (from site 3). a) 24-channel raw field record from the centre shot (shot location A); b) record from a) after bandpass filtering; c) 1-2 fold seismic section produced from the suite of five records obtained at the site; d) schematic representation of the source-receiver geometry used to collect the test site data.

The downhole shear wave velocities are examined in detail by Hunter et al. (2006). For post-glacial sediments, Figure 4(a) shows the compilation of interval velocities with depth Z (in metres) along with the best fitting curve given by:

$$V_S = 110.3 + 5.179*Z^{0.871} + -55.5 \text{ m/s } (2 \text{ sigma})$$
 (2)

A compilation of travel-time-weighted average shear wave velocities is shown in Figure 4(b). Hunter et al. (2006) recommend using a conservative estimate encompassing essentially all data, which is an empirical linear function given by:

$$V_{Sav} = 135 + 1.1667 * Z + -35 m/s$$
 (3)

Both equations are valid to a depth of 60 m.

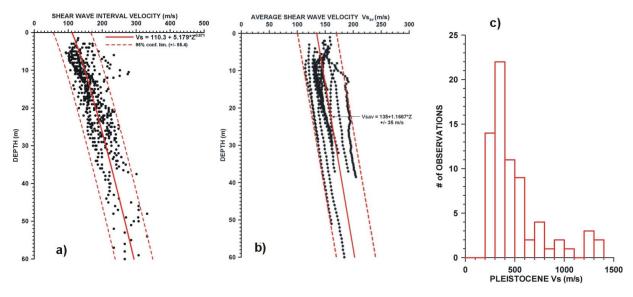


Figure 4: a) Best fit of interval Vs with depth for 18 boreholes in the Ottawa area. b) "Conservative" limits of travel-time-weighted average Vs from down-hole measurements. c) Distribution of down-hole Vs velocity measurements for glacial sediments; standard deviation of 277 m/s, median 298 m/s and the arithmetic mean is 503 m/s. After Hunter et al. (2006).

Glacial sediments were found at depth in some of the 18 boreholes. The results from 71 observations indicated that shear wave velocities in these sediments displayed a wide range of values which are thought to reflect the depositional environment (e.g. glaciofluvial gravels vs. tills). Figure 4(c) shows a histogram of the observations and associated statistics. The arithmetic mean of 503 m/s has been taken as a "typical" value for glacial sediments for calculations used in this paper.

Shear wave velocities of bedrock were not obtained in the immediate survey area. However, recent measurements (surface shear-wave refraction) in the Ottawa area consisting of 23 observations in similar Paleozoic rock yield an arithmetic mean value of 2380 m/s. This value is used for calculations in this paper.

Calculation of Vs₃₀ and NEHRP site classifications

Earthquake hazard maps were produced by combining the original borehole database with the additional information on the depth to bedrock and the thickness of post-glacial sediments obtained at the 100 seismic reflection sites. After applying the velocity functions described above to each of the geological units (bedrock, glacial and post-glacial sediments), grids and contour maps were created for Vs_{av}, Vs₂₀, Vs₃₀, Vs₄₀, and fundamental site periods. The data were modeled using Mapinfo Vertical Mapper Version 2.5. Grids and contours were created using the "natural neighbour" interpolation method. The gridding technique was set to honour local minimum and maximum values in the point file and not to aggregate data. This method allows the creation of accurate surface models from data sets that are very sparsely distributed or very linear in spatial distribution.

Results

Stratigraphic Variations

From combined borehole and geophysical data, maps of the bedrock elevation, thickness of glacial and post-glacial sediments, have been produced (Fig. 2).

The addition of the 100 seismic reflection sites has a profound effect on the understanding of the overall subsurface overburden structure. Figure 5 is a comparison between computer-contoured

thickness of post-glacial sediments with and without including these geophysical sites. A major change between the two maps can be seen in the central and eastern portions of the survey area. In particular, the map including the geophysical data (Fig. 5b) depicts three bedrock depressions that are not detected by the borehole data alone (Fig. 5a). The additional information provided by the seismic test sites in areas where the drift thickness reaches the greatest values (up to 187 m) was obtained at a fraction of the cost of drilling additional boreholes.

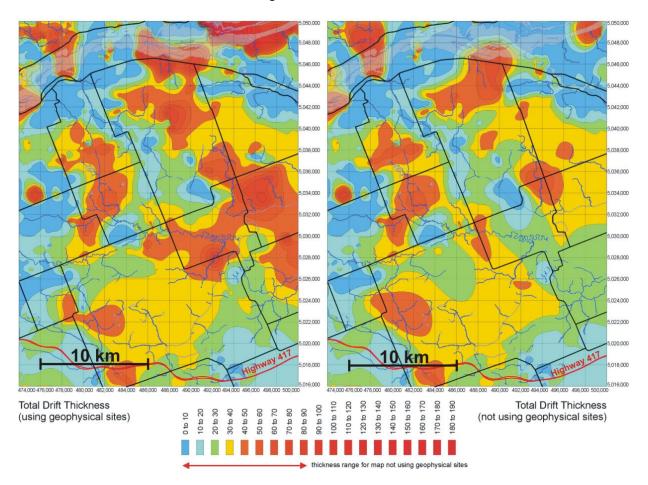


Figure 5: Maps of total drift thickness generated a) from the original borehole database and b) from the combined borehole and geophysical database (i.e. including results of 100 seismic test sites). The major difference is the definition of thicker drift areas in the eastern and central portions of the study area which were poorly defined using only the borehole database.

Average Shear Wave Velocities and NERHP Classifications

Figure 6b shows the NEHRP classification maps based on Vs_{30} determined from the subsurface geological data (from boreholes and seismic test sites) and derived shear wave velocity functions. Also shown in Figure 6 for comparison are the maps corresponding to the average shear wave velocity to 20 m depth (Vs_{20} , Fig. 6a) and to 40 m depth (Vs_{40} , Fig. 6c). The areal extent of zones characterized by average shear wave velocities >360 m/s (A, B, and C) are essentially constant in all three maps. These are the zones where high velocity bedrock and glacial sediments are encountered at shallow (<20 m) depth, and these materials then strongly bias the average shear wave velocity value. The occurrence of such large shear wave velocity contrasts at the basal part of the overburden and at the overburden-bedrock interface leads us to examine the choice of Vs_{30} as a standard. Where the soft post-glacial sediments are thick and make up essentially the entire depth range under consideration, the zones are mapped as classification D and E. Considering the average shear wave velocity of the upper 20 m (Fig.6a) results in much of the survey area in the <180 m/s

zone (equivalent to Zone E), whereas averaging the velocity over the upper 40 m (Fig. 6c) results in most of the area being in the 180-360 m/s zone (equivalent to Zone D). The implications of such variations are discussed below.

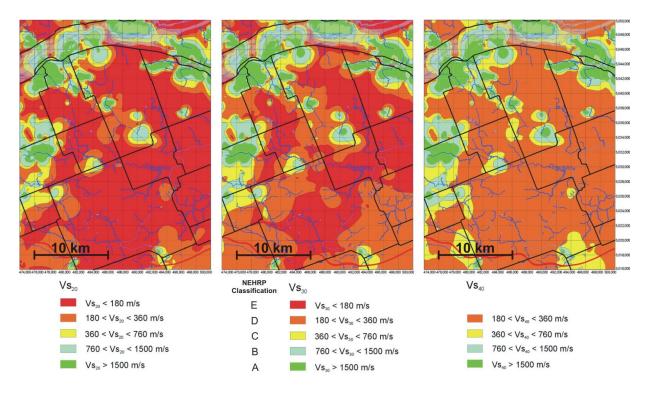


Figure 6: Maps of average shear wave velocity to depths of a) 20 m, b) 30 m, and c) 40 m.

Fundamental Site Period Estimation

The fundamental resonance period of a soft soil site is governed by the main seismic impedance contrast associated with the glacial-to-post-glacial or the post-glacial-to-bedrock boundary at depth. The fundamental site period is calculated from T=4Z/Vav where Z is the total thickness of post-glacial deposits and Vs_{av} is obtained from equation (3) substituting the total thickness Z in the equation. Figure 7a shows the distribution of Vs_{av} throughout the survey area. In general, Vs_{av} is low (in the 135-180 m/s range); Vs_{av} reaches values as high as 300 m/s only in areas of extremely thick post-glacial deposits, due to the gradual increase in shear wave velocity with depth. The fundamental site period map shown in Figure 7b indicates large variations up to 2.0 seconds that are associated with variations in the thickness of the post-glacial soft soils. Dark orange and red colours highlight zones where the site period exceeds 1 sec.

Discussion and Conclusions

The application of shallow seismic techniques in this study area has substantially improved the special coverage of ground truth data for the development of NEHRP zoning maps. In particular, the seismic data are able to provide data where borehole information is sparse because of thick, unconsolidated sediments.

The Vs_{30} criterion is used as a proxy for amplification factors regarding near-surface conditions in current building codes (Finn and Wightman, 2003). In our study area, the upper 30 m of thick post-glacial deposits is characterized by shear wave velocities that are less than 200 m/s. These low velocities lead to many areas defined as NEHRP classification E, where significant ground motion amplifications are expected with both short and long period amplification factors for

accelerations and ground velocities as high as 2:1. Whereas, for NEHRP class D, peak amplification factors only reach 1.3 and 1.4 for accelerations and ground motion velocities respectively

However, our study shows that the choice of total depth of soil for estimation of the average Vs can strongly affect the locations of zones D and E, without being associated with any major change in thickness of soft soils. Comparing Vs_{30} to Vs_{20} maps (Fig. 6), several areas shift from class D to E. This is due to the presence of a strong impedance contrast between 20-30 m depth (from a low velocity to a high-velocity unit). A reverse shift from D to E is seen when comparing Vs_{30} to Vs_{40} . A simple example of a 25 m thick post-glacial layer overlying bedrock serves to illustrate the problem: Vs_{20} would be 138 m/s (NEHRP E) whereas Vs_{40} would yield 215 m/s (NEHRP D). In other earthquake-prone soft soil regions of the world, where high-velocity bedrock occurs within 30 m of surface, it has been found that amplification factors based on NEHRP zones do not adequately estimate the ground response (Sun et al., 2005).

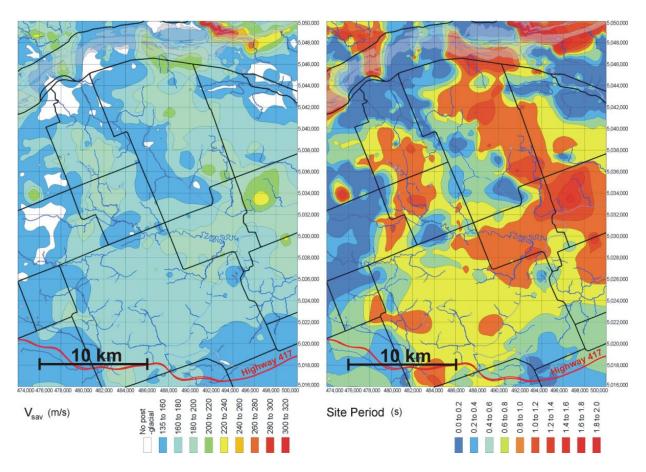


Figure 7: Maps of a) the average shear wave velocity to the base of the post-glacial sediments, and b) fundamental site periods (as defined in the text).

The soft soil total-depth factor can be more significant in earthquake amplification than near-surface effects shown on the Vs_{30} map. The fundamental site period map, obtained from the combination of variable bedrock depth and low average velocities, delineate areas where resonance effects of the earthquake waves could increase surface damage (Fig. 7b) if building structures exhibit natural periods that are in the same range. For example, a 10-storey building may have a natural period of 1 second and could be damaged in areas where the fundamental ground resonance period at 1 second can yield > 10 times amplification effect at 1 Hz.

An additional phenomenon of basin-edge induced waves may occur due to the highly complex bedrock topography as shown in Figure 2a. These may result in large amplitude interference effects from "trapped" Rayleigh and Love surface waves generated at basin edges and outcrops. To date, none of these thick soil and basin effects are addressed in the current NBCC.

The geological conditions of the study area extend to large populated areas of the Ottawa and St Lawrence Valleys wherever Champlain Sea deposits are found. The techniques developed here could be applied to large areas of the Ottawa-St. Lawrence Valley region of eastern Canada. The detailed surficial geological/geophysical model obtained for this study area could be used for waveform modelling studies that would provide important information about the propagation and amplification of earthquake waves within the different geological units and would consider both resonance and basin edge effects.

References

- Adams J., and Basham, P., 1989, The seismicity and seismotectonics of Canada east of the Cordillera, Geoscience Canada, v. 16, pp. 3-16.
- Adams and Halchuk, 2003, Fourth generation seismic hazard maps of Canada: Values for over 650 Canadian localities intended for the 2005 National Building Code of Canada. Geological Survey of Canada Open File 4459. 155 p. Available from http://seismo.nrcan.gc.ca
- Aki, 1988, Local site effects on strong ground motion, in Proc. Earthquake Engineering and Soil Dynamics II, Park City, Utah, June 27-30, pp. 103-155.
- Aki, 1993, Local site effects on weak and strong ground motion, Tectonophysics, v. 218, pp. 93-111.
- Aylsworth, J.M., Lawrence, D.E. and Guertin, J., 2000, Did two massive earthquakes in the Holocene induce widespread landsliding and near-surface deformation in part of the Ottawa Valley, Canada? Geology, v. 28, pp. 903-906.
- Belanger, J.R., 1998, Urban geology of Canada's National Capital Area, *in* Urban geology of Canadian cities. Karrow, P.F. and White, O.W., (eds.), Geological Association of Canada Special Paper 42: St. John's, Newfoundland, pp. 365-384.
- Building Seismic Safety Council (BSSC), 1998, 1997 Edition NEHRP Recommended Provisions for Seismic Regulations for New Buildings, FEMA 302/303, developed for the Federal Emergency Management Agency.
- Easton, R.M., 1991, The Grenville Province and the Proterozoic history of central and southern Ontario, In Geology of Ontario, Ontario Geological Survey, Special Volume 4, Part 1, pp. 715-904.
- Eden, W.J., Fletcher, E.B., and Mitchell, R.J., 1971, South Nation River landslide, 16 May 1971, Canadian Geotechnical Journal, v. 8, pp. 446-451.
- Evans, S.G. and Brooks, G.R., 1994, The earthflow in sensitive Champlain Sea sediments at Lemieux, Ontario, June 20 1993, and its impacts on the South Nation River, Canadian Geotechnical Journal, v. 31, pp. 384-394.
- Finn and Wightman, 2003, Ground motion amplification factors for the proposed 2005 editions of the National Building Code of Canada, Can. J. Civ. Eng., v. 30, pp. 272-278.
- Fulton, R.J. and Richard, S.H., 1987, Chronology of late Quaternary events in the Ottawa region. *in* Quaternary Geology of the Ottawa Region, Ontario and Quebec. Fulton, R.J. (ed.), Geological Survey of Canada, Paper 86-23, pp. 24-30.
- Gadd, N.R., 1986, Lithofacies of Leda clay in the Ottawa Basin of the Champlain Sea, Geological Survey of Canada, Paper 85-21, 44 p.
- Hunter, J.A., Benjumea, B., Harris, J.B., Miller, R.D., Pullan, S.E., Burns, R.A., and Good, R.L., 2002, Surface and downhole shear wave seismic methods for thick soil site investigations, Soil Dynamics and earthquake Engineering, v. 22, pp. 931-941.
- Hunter, J.A., Burns, R.A., Good, R.L., Aylsworth, J.M., Pullan, S.E., Perret, D., and Douma, M.,

- 2006, Borehole shearwave velocity measurements of Champlain Sea sediments in the Ottawa-Montreal region, Geological Survey of Canada, Open File, in press.
- NEHRP, 1994, Recommended provisions for seismic regulations of new buildings: Part I, provisions, FEMA 222A, National Earthquake Hazard Reduction Program, Federal, Emergency Management Agency, Washington, D.C.
- Sun, C.G., Kim, D.S., and Chung, C.K., 2005, Geologic site conditions and site coefficients for estimating earthquake ground motions in the inland areas of Korea, Engineering Geology, v. 81, pp. 446-469.
- Torrance, J.K., 1988, Mineralogy, pore-water chemistry, and geotechnical behaviour of Champlain Sea and related sediments, *in* The Late Quaternary Development of the Champlain Sea Basin, Gadd, N.R. (ed.), Geological Association of Canada, Special Paper 35, pp. 259-275.
- William, D.A. and Telford, P.G., 1986, Paleozoic geology of the Ottawa area, Geological Association of Canada, Mineralogical Association of Canada, Canadian Geophysical Union joint Annual Meeting, Ottawa '86, Field Trip 8 Guidebook, 25.p